NJC

Accepted Manuscript

DFT Study of Dihydrogen Addition to Molybdenum π-Heteroaromatic Complexes: Prerequisite Step for the Catalytic Hydrodenitrogenation Process

*Evgenii O. Fetisov,[a, b] Igor P. Gloriozov,[a] Denis A. Kissounko, *[c] Mikhail S. Nechaev, [a, d, e]*

*Samia Kahlal, [f] Jean-Yves Saillard, *[f] Yuri F. Oprunenko*[a]*

[a] Department of Chemistry, M.V. Lomonosov Moscow State University, Vorob'evy Gory, 119899 Moscow, Russia

[b] Department of Chemistry and Chemical Theory Center,

University of Minnesota, 207 Pleasant Street SE, Minneapolis, Minnesota 55455, USA

[c] Department of Science, Arapahoe Community College, 900 S. Santa Fe Drive, Littleton, Colorado, 80160.

[d] A. V. Topchiev Institute of Petrochemical Synthesis, Russian Academy of Sciences, Leninsky Prospect 29, Moscow, 119991 (Russia)

[e] N.D. Zelinsky Institute of Organic Chemistry, Russian Academy of Sciences, Leninsky prospect 47, Moscow, 119991 (Russia)

[f] Institut des Sciences Chimiques de Rennes, UMR 6226 CNRS-Universite de Rennes 1,

35042 Rennes cedex, France

1

Table of Content/Graphical Abstract

DFT Study of Dihydrogen Addition to Molybdenum η⁶-Heteroaromatic Complexes: Prerequisite Step for the Catalytic Hydrodenitrogenation Process

Evgenii O. Fetisov, Igor P. Gloriozov, Denis A. Kissounko, Mikhail S. Nechaev, Samia Kahlal, Yuri F. Oprunenko, Jean-Yves Saillard

Text: The mechanism proceeds via consecutive steps of oxidative H_2 addition, hydrogen metal-to-ligand transfer, accompanied by a change of metal-ligand hapticity.

2
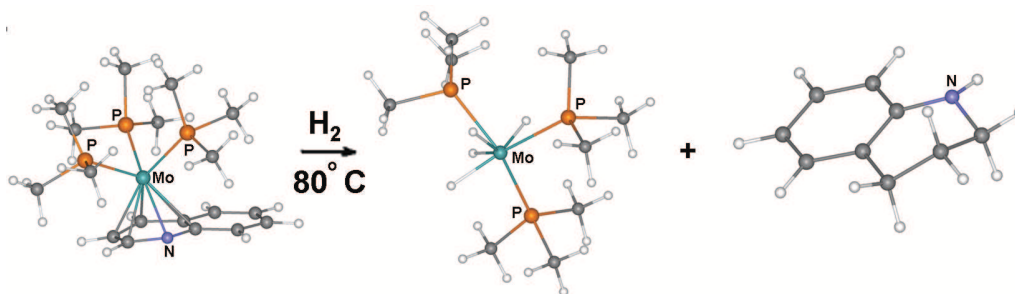
ABSTRACT. The range of molybdenum hydride complexes that are sought to participate in important catalytic hydrodenitrogenation process (HDN) of nitrogen containing polycyclic aromatic hydrocarbons were evaluated by DFT studies. The previously synthesized stable (η^6-quinoline)Mo(PMe$_3$)$_3$ complex **1N**, in which molybdenum is bonded to the heterocyclic ring, was chosen as a model. The hydrogenation of the quinone heterocycle, which was postulated as the initial step in the overall HDN reaction, is found to occur via three consecutive steps of oxidative addition of dihydrogen to Mo in **1N**. Successive transfers of hydrogen atoms from the metal to the heterocycle leads to the ultimate formation of the tetrahydrido molybdenum intermediate Mo(PMe$_3$)$_4$H$_4$ **13** and 2, 2, 3, 3-tetrahydroquinoline C$_9$H$_{11}$N **14**. All the involved intermediates and transition states have been fully characterized by DFT. This computational modeling of the hydrogenation of quinoline, as a part of extended HDN catalytic processes, provides a fundamental understanding of such mechanisms.

Introduction

Transition metal complexes play decisive role in transformation of simple organic substances and generation of important innovative derivatives such as technological precursors, materials for science, new polymers and medicines.[1] In recent years, the mechanisms of hydrodenitrogenation (HDN)[2] and hydrodesulfurization (HDS)[3] have gained considerable attention due to their relevance with respect to environmental aspects. Indeed, both processes are widely used in oil and coal industries to remove nitrogen- and sulfur-containing organic impurities in order to minimize subsequent pollution by NO$_x$ and SO$_x$, respectively. A great variety of transition and main group metal catalysts have been explored for the optimization of HDN and HDS reactions whereas molybdenum complexes proved to be one of the most efficient catalysts.[4] Typically, such reactions involve reversible σ- and/or π-coordination of an

heterocyclic organic molecule, followed by consecutive cycles of dihydrogen addition/hydride-to-ligand transfer, to produce hydrogenated derivatives of the heterocyclic molecule which possesses weaker C-N (or C-S) bonding than its corresponding aromatic heterocycles with the tendency to abstract heteroatom-containing parts.[5,6] For condensed aromatic systems, the metal moiety in these more or less stable complexes often undergoes so-called intra-molecular inter-ring haptotropic rearrangements (IRHR), which can be degenerative $\eta^6 \rightleftharpoons \eta^6$ or non-degenerative $\eta^6 \rightleftharpoons \eta^5$, $\eta^1 \rightleftharpoons \eta^5$, or $\eta^1 \rightleftharpoons \eta^6$.[7] In the course of such rearrangements, the metal and its ancillary ligands move reversibly or irreversibly along the polyaromatic ligand from one ring to another one. Such reactions are considered to be plausible processes during the HDN/HDS reactions transferring hydrogen atoms both to carbocyclic and heterocyclic rings.

Examples of haptotropic rearrangements for polyaromatic carbocyclic ligands, such as naphthalene, biphenyl, biphenylene, indene, fluorene, phenanthrene, anthracene,[8] and more recently coranullene,[9] coronene,[10] fullerenes,[11] carbon nanotubes,[12] and graphenes,[13] are quite abundant. However, related examples of rearrangements involving heterocyclic analogues are far less common. Earlier examples with group VI metals were proposed and then demonstrated by carbazole[14] and dibenzothiophene[15] complexes. Such complexes as well as other labile transition metal complexes could be considered as prospective catalysts of hydrogenation and HDN/HDS due to the reduced metal hapticity in the course of IRHR and, as a result, the ability to coordinate exogeneous additional organic molecule and dihydrogen for further transformations. For example, a series of rhodium complex with pentamethylcyclopentadienyl and cyclooctadiene ancillary ligands were already reported to catalyze the hydrogenation of quinoline[16] to the corresponding fully hydrogenated derivatives by means of consecutive dihydrogen addition/hydride transfer cycles.[17]

Recently Parkin *et al.* reported the synthesis of a series of η^6-quinoline, isoquinoline and

quinoxaline (illustrated in Scheme 1 for quinoline) molybdenum complexes, as well as related

η^6- and η^5-indolyl and carbazolyl molybdenym complexes.[18,19,20] In these complexes, the metal

can coordinate through a carbocyclic as well as an heterocyclic ring and undergoes series of σ, π

$\eta^1 \rightleftharpoons \eta^6$ and π, π $\eta^6 \rightleftharpoons \eta^6$ inter-ring haptotropic rearrangements (IRHR), which can be

induced both thermally and photochemically. Such complexes have very good prospects for

HDN/HDS processes under molybdenum catalysis.
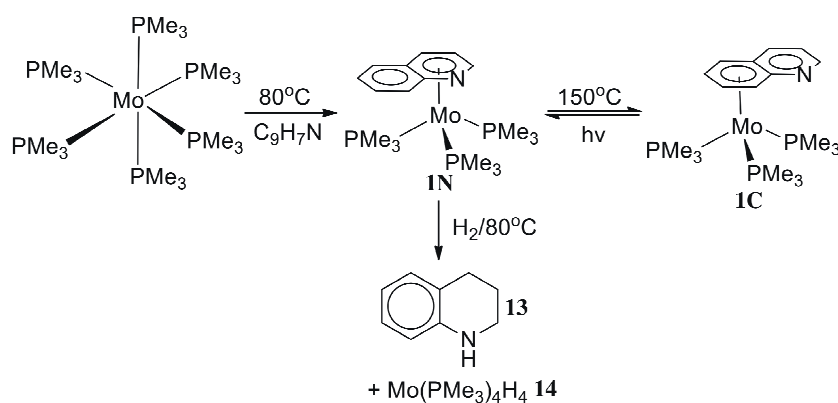
Scheme 1. Synthesis, hydrogenation and haptotropic rearrangements of η^6-quinoline

molybdenum complexes

The ability of the molybdenum moiety to undergo IRHR between carbo- and heterocyclic rings

for complexes of different hapticities was unambiguously demonstrated. Either ring could be

potentially activated for subsequent catalytic hydrogenation depending on the reaction

conditions. Thus, complex **1N** with η^6-coordination of molybdenum on heterocyclic ring reacts

with dihydrogen under very mild conditions (80°C, and atmospheric pressure) to form ultimately

the tetrahydrido molybdenum derivative Mo(PMe3)4H4 **13** and the saturated heterocyclic

molecule C9H11N **14**. Some of the hydridic reactive intermediates that are believed to play

pivotal role in the overall catalytic HDN process were isolated and characterized by Parkin,[18,19] whereas other intermediates remained elusive. Alternative complex **1C** with η^6-coordination of molybdenum on the carbocyclic ring could also principally participate in hydrogenation and HDN processes, but it should be noted that partial or full hydrogenation of complex **1C** was not reported and no experimental data on any hydrogenation product with hydrogen localization on carbocyclic ring have been reported.[18,19] This could be explained by the fact that a carbocyclic ring of an heteropolycyclic ligand is harder to hydrogenate than an heterocyclic ring under the conditions of catalytic hydrogenation.[7] Moreover, these data are in accordance with the fact that a carbocyclic analog of **1N**, namely the naphthalene complex $(\eta^6\text{-}C_{10}H_8)Mo(PMe_3)_3$, failed to react with dihydrogen, while the anthracene relative $(\eta^6\text{-}C_{14}H_{10})Mo(PMe_3)_3$ reacts somehow with dihydrogen but adds only one H_2 molecule to Mo, forming an η^4-*dihydrido* complex rather than further products with hydrogen transfer on carbocyclic ring. This phenomenon was called "anthacene effect".[21]

In this work, we investigate by the means of density functional theory (DFT) calculations the mechanism of the catalytic hydrogenation of a molybdenum complex, which is obviously a crucial part of the more complex HDN reaction under molybdenum catalysis. The quinoline complex **1N** depicted in Scheme 1 was chosen initially as a model for our calculations because it easily hydrogenated, giving **14**.

Computational details

DFT calculations were performed at the Joint Supercomputer Center (JSCC) (Moscow) with the use of the PRIRODA-04 program written by Laikov.[22] The PBE functional[23] was considered together with the TZV2p three-exponential basis set of Gaussian-type functions for valence

electrons[22] (basis set specification: {3,1}/{5,1} for H, {3,3,2}/{5,5,2} for C, N, and P and {5,5,4}/{9,9,8} for Mo), associated with the SBK-JC relativistic pseudopotential[24,25] for all core electrons. Such level of calculations, which is a good compromise between computational accuracy and calculation expenditures, was previously demonstrated to exhibit good results for geometry and energy parameters of transition metal complexes with polyaromatic ligands in general.[15,26] Moreover, test calculations on both **1N** and **1C** provided optimized geometries which were very close to their X-ray structures[18] (see Figure 1; additional computed data are presented in SI). Stationary points were identified by analyzing Hessians. Hapticities of the stationary and transition states were deduced from bond distances and bond orders. Stationary point energies (*E*) are given with corrections for zero-point vibrations. The thermodynamic functions (Gibbs energies, *G*) at 298.15 K were calculated using statistical rigid rotator–harmonic oscillator equations. The conjugation of the observed transition states with the corresponding potential energy surface minima was checked by constructing internal reaction coordinates (IRC).
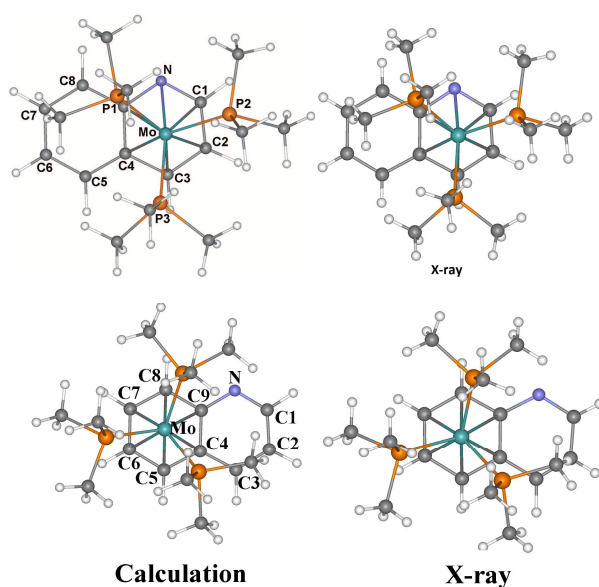

Figure 1. Calculated and X-ray[18] structures of the complexes **1N** and **1C**

Results and Discussion

The mechanism of hydrogenation of **1N** (Scheme 1) was modeled starting from the *pre-reaction van der Waals complex* of **1N** with a dihydrogen molecule, labeled **1-N** (**1N** = **1N**···H_2). The schematic energy diagram of this multistep process into the post-reaction complex **12-N**, including all intermediates and transition states is presented in Figure 2. Conventional schematic description of the stable complexes **1N**-**12-N** structures are presented in Scheme 2 and their 3D geometries in Figure 3. The 3D geometries of the associated transition states are shown in Figure 4 and additional computed data are provided in the SI. The process occurs via consecutive dihydrogen addition/hydride transfer steps to yield the final σ-complex **12-N** which decomposes without any activation barrier into $Mo(PMe_3)_4H_4$ (**13**) and 2, 2, 3, 3-tetrahydroquinoline $C_9H_{11}N$, **14**. The free Gibbs energy of **13** + **14** is lower than that of **12-N** by 4.4. kcal/mol. Thus, the reaction of full hydrogenation of **1N** into **13** + **14** is exothermic ($\Delta\Delta G$ = -9.7 kcal/mol). Similar mechanistic and thermodynamic results were previously observed for the hydrogenation of pyridine on a molybdenum(III) phosphide surface.[27]
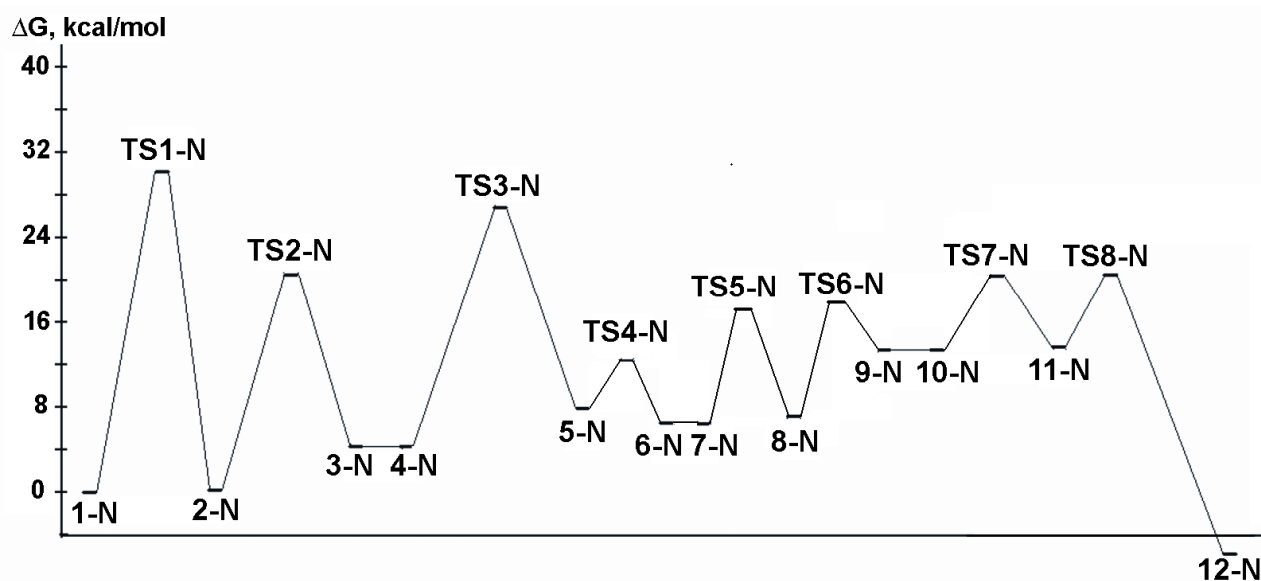

Figure 2. Computed energy diagram for the **1N** hydrogenation process.

Table 1. Stationary states energies, E (a.u.), ΔE (kcal/mol) and ΔG (kcal/mol) for the hydrogenation process of in **1N**.[a]

Structure	E	ΔE	ΔG
1-N	-221.305646	0	0
TS1-N	-221.266677	24.5	*30.4*
2-N	-221.314831	-5.8	0.1
TS2-N	-221.282729	14.4	20.6
3-N	-221.312854	-4.5	4.0
4-N	-222.479606	-4.5	4.0
TS3-N	-222.450713	13.6	26.8
5-N	-222.489090	-10.5	7.5
TS4-N	-222.480408	-5.0	11.1
6-N	-222.492068	-12.3	5.1
7-N	-223.660900	-12.3	5.1
TS5-N	-223.650260	-5.6	17.2
8-N	-223.673569	-20.2	5.8
TS6-N	-223.651179	-6.2	17.9
9-N	-223.662892	-13.5	13.9
10-N	-224.823146	-13.5	13.9
TS7-N	-224.818938	-10.9	20.3
11-N	-224.837256	-22.4	13.4
TS8-N	-224.822544	-13.1	20.4
12-N	-224.866945	-41.0	-5.3

[a] **1-N→3-N**: first H_2 addition process; **4-N→6-N**: second H_2 addition process; **7-N→9-N**: third H_2 addition process; **10-N→12-N**: fourth H_2 addition process. To obtain a correct diagram with increasing the number of H_2 molecules along the course of the hydrogenation process, relative energies were corrected in such a manner that the last structure of the previous hydrogenation step and the first structure of the next step are consider as having same relative energies.
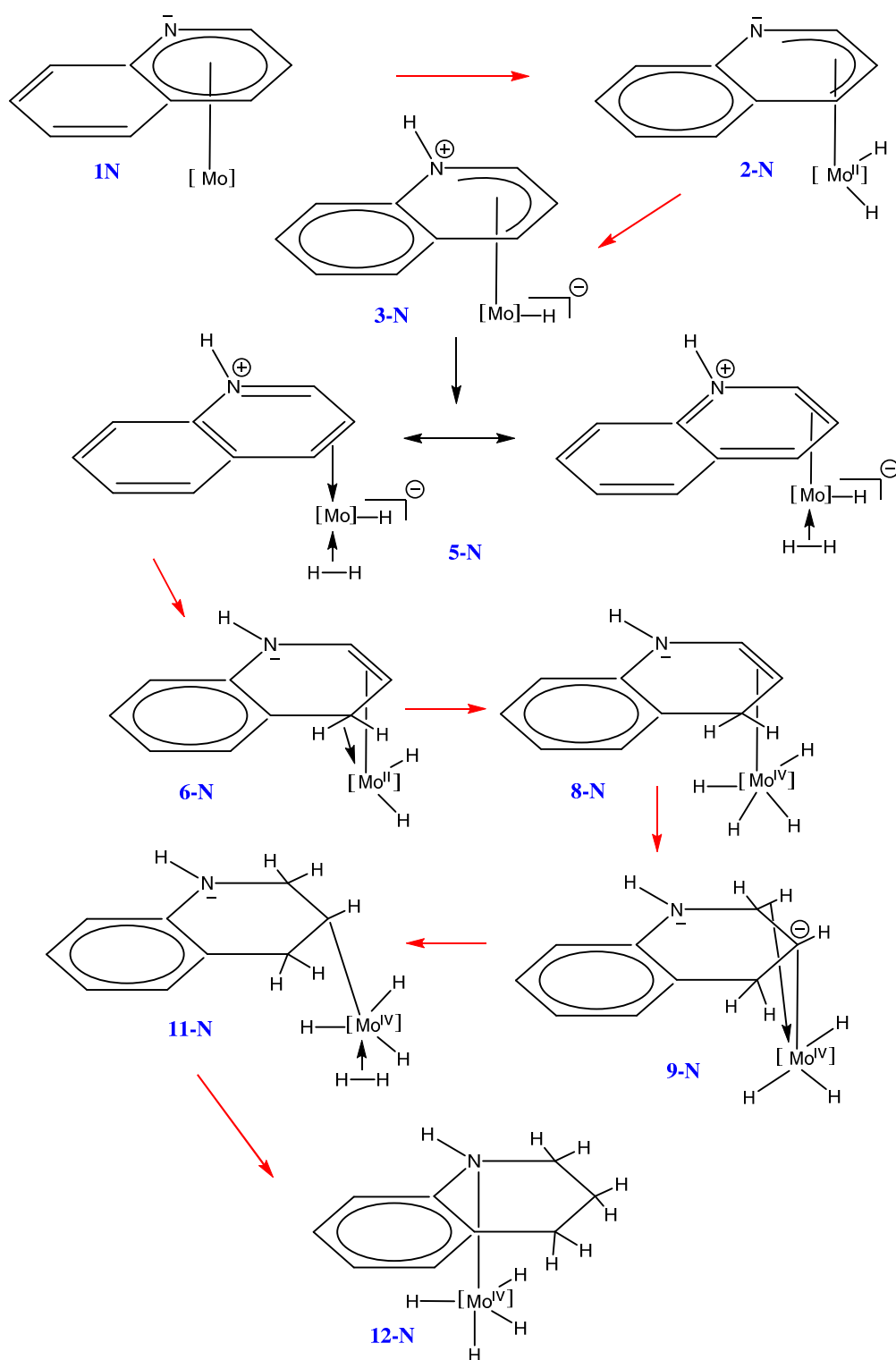
Scheme 2. Conventional schematic description of the energy minima involved in the mechanism of Figure 2 ([Mo] = Mo(PMe₃)₃) .
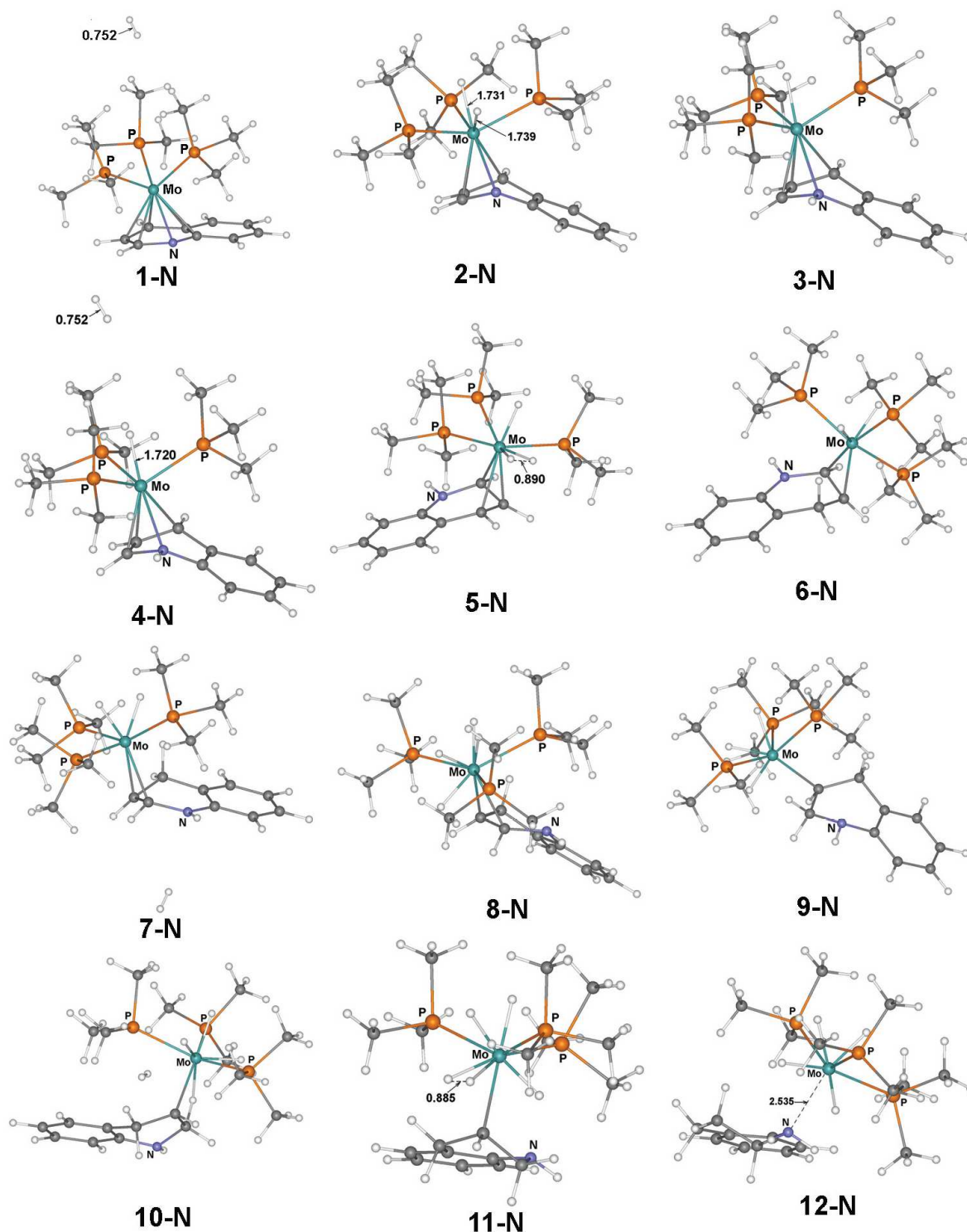
Figure 3. Optimized 3D geometries of the stable species involved in the hydrogenation process of **1N** (Note that structures of **3-N** and **4-N, 6-N** and **7-N, 9-N** and **10-N** differ from each other by the addition of one H₂ molecule to the formers, thus forming pre-reaction *van der Waals* complexes **4-N, 7-N and 10-N**, respectively; see also Figure 2).
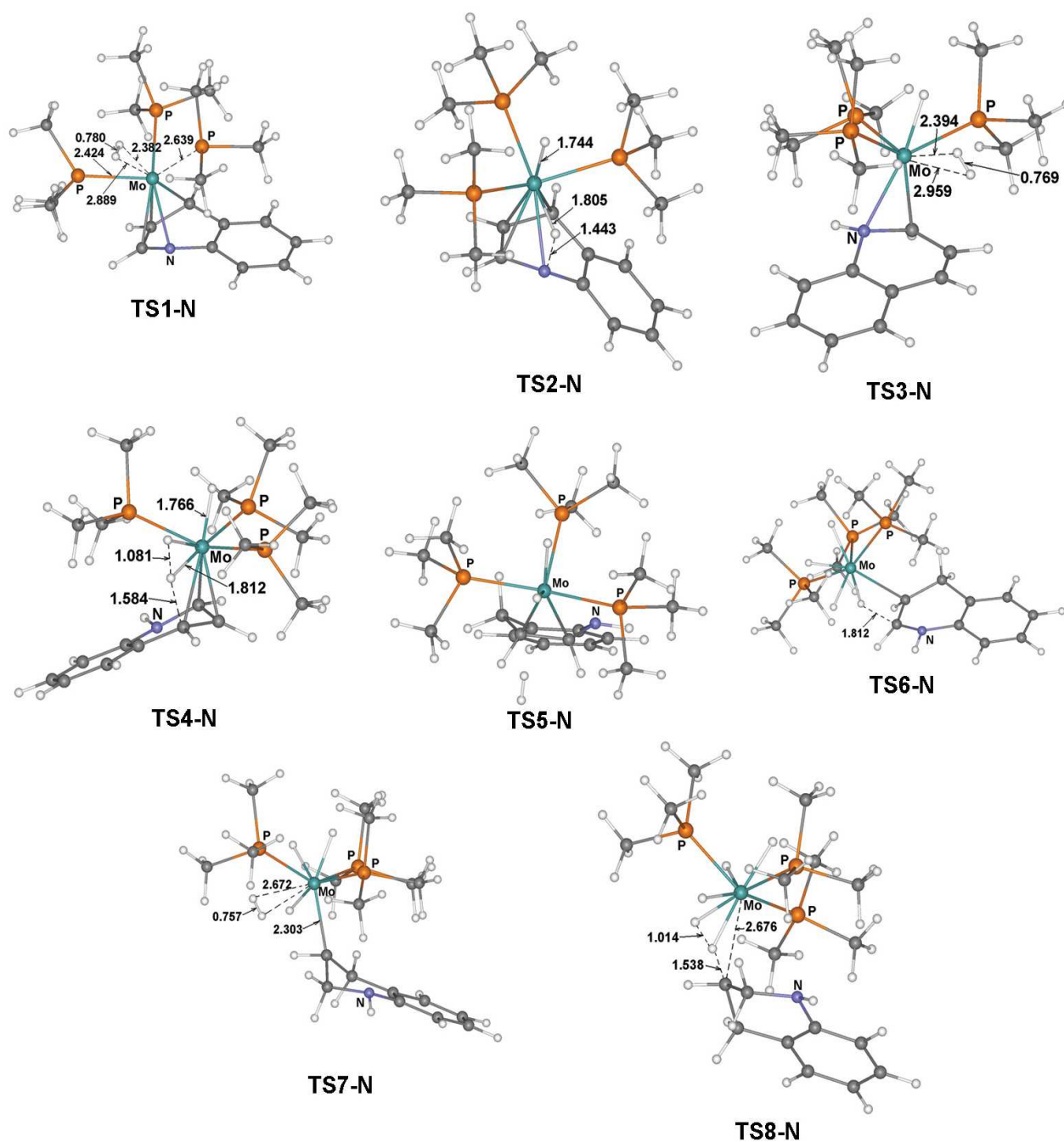
Figure 4. Optimized 3D geometries of the transition states involved in the hydrogenation process of **1N** (see Figure 2).

In the first stage one molecule of H$_2$ adds to complex **1N** via a Kubas-type transition state **TS1-N** with an activation barrier ΔG=30.4 kcal/mol. The dihydrogen character of **TS1-N** is evidenced by

the Mo-H distances of 2.382Å and 2.889Å and the only slightly elongated H-H distance 0.780Å

which compares well with similar values in other dihydrogen complexes on the basis of DFT and

X-ray.[28] **TS1-N** leads to the dihydride intermediate **2-N**, with Mo-H and H-H distances of 1.731Å

and 1.859Å, respectively. These distances are similar to those found in other dihydride complexes

both from experimental or theoretical analyses.[28] In order to maintain its 18-electron

configuration, the molybdenum atom in **2-N** is shifted towards tetrahapto configuration of the

heterocycle which, as a result, is now bent (torsion angle between two planes 147°).

Unsurprisingly, this partial quinoline decoordination is largely preferred over PMe$_3$ dissociation.

The next step consists in the shifting of one of the metal-bonded hydrogens onto the nitrogen

atom, leading to the formation of **3-N.** Formally, this is a simple proton transfer associated with a

formal 2-electron reduction of the metal (Scheme 2), and therefore the 18-electron configuration

of the metal is maintained. The formation of **3-N** proceeds with an activation barrier ΔG=20.6

kcal/mol through the transition state **TS2-N**, in which one hydrogen keeps bonded the metal and

the second one occupies a bridging position between Mo and N (N-H=1.443Å, Mo-H=1.805Å,

Mo-N=2.336Å, Mo-N-H=64.4°). The terminal M-H bond distance in **TS2-N** is 1.744 Å, in good

agreement with comparable distance in dihydride complexes.[28]

The addition of the second H$_2$ molecule proceeds into two steps. In the first one, the Kubas-type

intermediate **5-N** is formed (H-H=0.890 Å, Mo-H=1.828 Å and 1.832 Å) through the transition

state **TS3-N**. In **5-N** the metal is bonded to only three atoms of the heterocycle (C1, C2 and C3)

whereas it was bonded to four atoms (N, C1, C2 and C3) in **3-N** (see atom numbering in Figure

1). The corresponding Mo-C distances are 2.327 Å, 2.193 Å and 2.401 Å, for C1, C2 and C3,

respectively. In such a *trihapto* coordination, a 6-membered aromatic cycle cannot provide to the

metal with more than 2 electrons, so that the bonding is best described with the two limit structure

shown in Scheme 2. Hence, **5-N** is, as well as **3-N**, an 18-electron Mo^0 complex. The following

step consists in the migration of one of the H_2-coordinated atom onto C3 (formally a hydride transfer associated with a 2-electron oxidation of the metal (Scheme 2)), leading to the formation of the Mo^{II} dihydrido complex **6-N** in which the heterocycle is now η^2-coordinated to the metal through C1 and C2, with Mo-C distances of 2.322 Å and 2.185 Å, respectively. Interestingly, the newly built C3-H bond in **6-N** (C-H = 1.180 Å) makes an agostic bond to Mo (Mo-H = 2.014 Å; Mo-C3 = 2.533 Å), allowing the Mo^{II} center to maintain its 18-electron configuration.

In the following stage, a third entering H_2 molecule easily displaces the weak agostic bond in **6-N**, and oxidatively adds to the metal, leading to the 18-electron Mo^{IV} complex **8-N**, which, similarly as in the formation of **6-N** from **5-N**, transfers one hydride atom on the heterocycle (onto C1), leading to an η^1-coordination of quinoline (Mo-C2 = 2.294 Å). The resulting trihydrido Mo^{IV} **9-N** complex maintains its 18-electron configuration through the building of an agostic C1-H bond (Mo-H = 1.961 Å, Mo-C1 = 2.516 Å and C1-H = 1.194 Å). The addition of the fourth H_2 molecule proceeds in a more or less similar way as the third one: formation of the 18-electron Kubas-type Mo^{IV} complex **11-N** from displacement of the C-H agostic bond, followed by hydrogen migration onto the heterocycle leading to the formation of the tetrahydro complex **11-N**. Noteworthy, this last step is accompanied with an haptotropic η^1, η^1 rearrangement (**TS8-N→12-N**) via an Mo [1,3]-shift from C2 to N. This transition is mainly responsible for the overall exothermic effect of the whole heterocyclic ring hydrogenation process of **1N**.

The highest activation barrier of the whole process from **1N** to **13** + **14** (Figure 2) occurs for the first H_2 addition process (formation of transition state **TS1-N** with ΔG=30.4 kcal/mol) which is similar to the value associated with IRHR of chromium tricarbonyl on monosubstituted naphthalenes (ΔG=30 kcal/mol).[7] Interestingly, our investigated hydrogenation reaction proceeds at similar temperatures (80°-90°C) as IRHR in naphthalene complexes.[15] This means that in the

course of the hydrogenation process, different η^n,η^n-IRHR could occur when the organometallic moiety migrates from the intact or partially hydrogenated heterocyclic ring to the carbocyclic ring, leading incidentally to a possible hydrogenation of the carbocyclic ring. However, this process usually occurs in much harder experimental conditions than the hydrogenation of the heterocyclic ring.[7]

Conclusions

In conclusion, we have unambiguously shown that the hydrogenation of a quinoline ligand coordinated to molybdenum via its heterocyclic ring is possible. The mechanism proceeds by consecutive steps of oxidative hydrogen addition, hydride metal-to-carbon/nitrogen transfer, accompanied by a change of the metal-ligand coordination mode. After the fourth hydrogenation step, the free tetrahydroquinoline molecule **12** stays η^1-coordinated to molybdenum. This type of mechanism is very likely to be relevant in the ultimate hydrodenitrogenation process of quinoline or related nitrogen-containing ligands by molybdenum-based organometallic catalysts through the initial formation of an η^6-complex.

ASSOCIATED CONTENT

Supporting Information. The complete tables of optimized molecular geometries, atomic coordinates, and important bond distances for all intermediates and transition states are available in supporting information.

AUTHOR INFORMATION

Corresponding Author

* a. Dr. Yuri F. Oprunenko. E-mail: *oprunenko@org.chem.msu.ru*

* b. Jean-Yves Saillard. E-mail: *jean-yves.saillard@univ-rennes1.fr*

* c. Dr. Denis A. Kissounko. E-mail: *denis.kissounko@arapahoe.edu*

ACKNOWLEDGMENT

REFERENCES

1. V. P. Ananikov, E. A. Khokhlova, M. P. Egorov, A. M. Sakharov, S. G. Zlotin, A. V. Kucherov, L. M. Kustov, M. L. Gening and N. E. Nifantiev, *Mendeleev Commun.*, 2015, **25**, 75.

2. N. Escalona, J. Ojeda, R. Cid, G. Alves and L. A. Agudo, *Appl. Cat. A: Gen.*, 2002, **234**, 45.

3. J. Quartararo, S. Mignard and S. Kasztelan, *J. Catal.*, 2000, **192**, 307.

4. J. Raty and T. A. Pakkanen, *Catal. Lett.*, 2000, **65**, 175.

5. V. A. Sal'nikov, P. A. Nikul'shin and A. A. Pimerzin, *Petrol. Chem.*, 2013, **53**, 233.

6. K. Weissermel and H.-J. Arpe, *Industrial Organic Chemistry*, Wiley-VCH, Weinheim, 4th edn, 2003.

7. C. Bianchini, A. Meli and F. Vizza, *Eur. J. Inorg. Chem.*, 2001, 43.

8. Yu. F. Oprunenko, *Russ. Rev.*, 2000, **69**, 683 and references therein.

9. M. W. Stoddart, J. H. Brownie, M. C. Baird and H. L. Schmider, *J. Organomet. Chem.*, 2005, **690**, 3440.

10. H. Sato, C. Kikumori and S. Sakaki, *Phys. Chem. Chem. Phys.*, 2011, **13**, 309.

11. W. D. Harman and H. Taube, *J. Am. Chem. Soc.*, 1987, **109**, 1883.

12. F. Nunzi, F. Mercuri, F. De Angelis, A. Sgamellotti, N. Re and P. Giannozzi, *J. Phys. Chem. B*, 2004, **108**, 5243.

13. F. Nunzi, F. Mercuri and A. Sgamelotti, *Mol. Phys.*, 2003, **101**, 2047.

14. K. Shen, X. Tian, J. Zhong, J. Lin, Y. Yi Shen and P. Wu, *Organometallics*, 2005, **24**, 127.

15. Yu. F. Oprunenko, I. P. Gloriozov, *J. Organomet. Chem.*, 2009, **694**, 1195.

16. W. B. Wang, S. M. Lu, P. Y. Yang, X. W. Han and Y. G. Zhou, *J. Am. Chem. Soc.*, 2003, **125**, 10536.

17. T.-G. Zhou, *Acc. Chem. Res.*, 2007, **40**, 1357 and references therein.

18. G. Zhu, J. M. Tanski, D. G. Churchill and G. Parkin, *J. Am. Chem. Soc.*, 2002, **124**, 13658.

19. G. Zhu, K. Pang and G. Parkin, *J. Am. Chem. Soc.*, 2008, **130**, 1564.

20. A. Sattler, G. Zhu and G. Parkin, *J. Am. Chem. Soc.*, 2009, **131**, 7828.

21. A. Stanger and H. Weismann, *J. Organomet. Chem.*, 1996, **515**, 183.

22. D. N. Laikov and Yu. A. Ustynyuk, *Russ. Chem. Bull.*, 2005, **54**, 820.

23. J. P. Perdew, K. Burke and M. Ernzerhof, *Phys. Rev. Lett.*, 1996, **77**, 3865.

24. W. J. Stevens, H. Basch and M. Krauss, *J. Chem. Phys.*, 1984, **81**, 6026.

25. T. R. Cundari, and W. J. Stevens, *J. Chem. Phys.*, 1993, **98**, 5555.

26 a) Yu. F. Oprunenko and I. P. Gloriozov, *Russ. Chem. Bull.*, 2010, **59**, 2061; b) Yu. F. Oprunenko and I. P. Gloriozov, *Russ. J. Phys. Chem. A*, 2012, **86,** 979.

27. Y. Li, W. Guo, H. Zhu, L. Zhao, M. Li, S. Li, D. Fu, X. Lu and H. Shan, *Langmuir*, 2012, **28**, 3129.

28. a) M. Baya, B. Eguillor, M. A. Esteruelas, A. Lledós, M. Oliván and E. Oñate, *Organometallics*, 2007**, 26***, 5140; b) C.-F. Huo, Y.-W. Li, M. Beller and H. Jiao, *Organometallics*, 2004, **23**, 2168.

Table of Content/Graphical Abstract

DFT Study of Dihydrogen Addition to Molybdenum η^6-Heteroaromatic Complexes: Prerequisite Step for the Catalytic Hydrodenitrogenation Process

Evgenii O. Fetisov, Igor P. Gloriozov, Denis A. Kissounko, Mikhail S. Nechaev, Samia Kahlal, Yuri F. Oprunenko, Jean-Yves Saillard

Text: The mechanism proceeds via consecutive steps of oxidative H_2 addition, hydrogen metal-to-ligand transfer, accompanied by a change of metal-ligand hapticity.